Breakup reaction study of the Brunnian nucleus ^{10}C

N. Curtis, N.L. Achouri, N.I. Ashwood, H.G. Bohlen, W.N. Catford, N.M. Clarke, M. Freer, P.J. Haigh, B. Laurent, N.A. Orr, et al.

Breakup reaction study of the Brunnian nucleus ^{10}C

N. Curtis,[1,*] N.L. Achouri,[2] N.I. Ashwood,[1] H.G. Bohlen,[3] W.N. Catford,[4] N.M. Clarke,[1] M. Freer,[1] P.J. Haigh,[1] B. Laurent,[2] N.A. Orr,[2] N.P. Patterson,[4] N. Soić,[5] J.S. Thomas,[4] and V. Ziman[1]

[1]*School of Physics and Astronomy, University of Birmingham, Edgbaston, Birmingham, B15 2TT, UK.*
[2]*LPC-ENSICAEN, IN2P3-CNRS et Université de Caen, F-14050 Caen Cedex, France.*
[3]*Hahn-Meitner-Institut GmbH, Glienicker Str. 100, 14109 Berlin, Germany.*
[4]*School of Electronics and Physical Sciences, University of Surrey, Guildford, Surrey, GU2 7XH, UK.*
[5]*Rudjer Bošković Institute, Department of Experimental Physics, Bijenička 54, HR-10000 Zagreb, Croatia.*

The structure and $2\alpha + 2p$ breakup of ^{10}C, the only known Brunnian nucleus, has been studied at 33.3 MeV/nucleon. The breakup kinematics were used to reconstruct the $^{10}\mathrm{C} \rightarrow {}^{9}\mathrm{B} + p$, $^{9}\mathrm{B} \rightarrow {}^{8}\mathrm{Be} + p$, $^{8}\mathrm{Be} \rightarrow \alpha + \alpha$ and $^{10}\mathrm{C} \rightarrow {}^{6}\mathrm{Be} + \alpha$, $^{6}\mathrm{Be} \rightarrow {}^{5}\mathrm{Li} + p$, $^{5}\mathrm{Li} \rightarrow \alpha + p$ decay paths. Proton emission was seen to be favored. The decay of excited states at $\mathrm{E_x} = 4.20$, 5.31 and 6.74 MeV was observed. The previously unobserved state at 4.20 MeV may correspond to a $\mathrm{J}^{\pi} = 0^{+}$ α+2p+α cluster structure.

PACS numbers: 23.50.+z, 23.60.+e, 25.60.-t, 27.20.+n

The Borromean systems have been the subject of much interest in recent years. These are a class of nuclei that may be described in terms of a three-body structure, with the property that the removal of any one of the three constituents results in an unbound two-body subsystem [1]. Perhaps the best known example is ^{11}Li, which is believed to possess a dominant ^{9}Li+n+n structure in its ground state. The two-body subsystems, ^{10}Li (^{9}Li+n) and the di-neutron (n+n), are unbound by 25 and 66 keV respectively. All three bodies are therefore required to produce the overall bound nuclear system. As such the structure of the Borromean nuclei provides a stringent test of nuclear few body models.

There is only one known example of a four-body nucleus that has Borromean-like properties: ^{10}C, which may be described as α+α+p+p. This nucleus has the property that the removal of any one of the four constituents results in an unbound three-body system. The removal of a proton from ^{10}C leads to ^{9}B, which is unbound to ^{8}Be+p decay by 185 keV. The removal of an α-particle produces ^{6}Be. Although the Q-value for ^{5}Li+p decay is -595 keV, ^{6}Be is unbound to this channel due to the $\sim$1.5 MeV width of the ^{5}Li ground state. In addition, the removal of any two particles from ^{10}C results in an unbound two-body system. The removal of both protons produces ^{8}Be (unbound to α+α decay by 92 keV), one α-particle and one proton results in ^{5}Li (unbound to α+p decay by 1967 keV) and the removal of both α-particles would produce the di-proton (unbound to p+p decay by 93 keV). All four constituents must be present to bind the system, and ^{10}C may therefore be described as a "Super-Borromean" nucleus. In fact ^{10}C is the only known nuclear example of a 4^{th} order Brunnian link [2], a nontrivial link in knot theory that becomes trivial if any component is removed. Three-body Borromean nuclei are examples of 3^{rd} order Brunnian links.

The aim of this experiment was to study the spectroscopy of ^{10}C and to determine the relative strengths of the α and proton decay channels: $^{10}\mathrm{C} \rightarrow {}^{9}\mathrm{B} + p$, $^{9}\mathrm{B} \rightarrow {}^{8}\mathrm{Be} + p$, $^{8}\mathrm{Be} \rightarrow \alpha + \alpha$ and $^{10}\mathrm{C} \rightarrow {}^{6}\mathrm{Be} + \alpha$, $^{6}\mathrm{Be} \rightarrow {}^{5}\mathrm{Li} + p$, $^{5}\mathrm{Li} \rightarrow \alpha + p$. The experiment was performed at the GANIL accelerator facility. A 33.3 MeV/nucleon ^{10}C beam was produced following the fragmentation of a 60 MeV/nucleon ^{12}C primary beam in a 3 mm thick Be production target. The secondary beam was purified to 98.6 % ^{10}C using the LISE3 spectrometer and had an average intensity of 2.5×10^4 particles per second. The beam contaminants (observed in the detector telescope) were d (0.2 %), ^{3}He (0.3 %) and ^{4}He (0.9 %) at 24.2, 40.4 and 22.3 MeV/nucleon respectively (corresponding to the same magnetic rigidity as the ^{10}C). The beam was not identified on an event by event basis, but as the contaminants were all light particles they could not give rise to the multiple proton and α-particle channels of interest. The contaminants were only observed in singles events in the detector array, and not in double, triple or quadruple coincidences. Therefore the ^{4}He contaminant did not contribute to the detection of α-particles from any of the breakup channels considered. The beam was tracked onto the reaction target (20, 45 and 95 mg/cm^2 ^{12}C foils were used) on an event by event basis using a position sensitive drift chamber. A 5 mm thick, 10 mm diameter, Ta beam stop was positioned 106 mm (downstream) from the target. This protected the detector telescope, which was placed at 0° (on the beam axis), from the direct and small angle scattered ^{10}C beam. The beam stop was held in place by a 3 mm diameter rod.

The detector telescope consisted of four separate elements, each (50×50) mm^2 in active area. The first two elements, at 123 and 130 mm from the target respectively, were silicon resistive strip detectors (RSD). Each RSD was 500 μm thick and segmented into 16 independent 3 mm wide strips. Resistive charge division provided position information along the strip length. The strips on the front detector (RSD1) were vertical and those on the second (RSD2) horizontal. The third element was a

1000 μm thick silicon double sided strip detector (DSSD) placed 148 mm from the target. This was segmented into 32 independent 3 mm wide strips, with 16 horizontal strips on the front face and 16 vertical strips on the back face. The final element, 160 mm from the target, was an array of 64 CsI scintillators, each 20 mm thick and with an area of (6 × 6) mm^2. The effective solid angle covered by the array, calculated as the difference between the coverage of the CsI detectors and the beam stop and mounting rod, was 85 msr. Used in combination, the four detectors provided ΔE-E particle identification with isotopic separation for H, He and Li ions. The highly segmented nature of the array allowed all four particles from the decay of ^{10}C (α+α+p+p) to be detected in coincidence. Position resolution for the α-particles was $\sim$ 1 mm (FWHM) in both X and Y (provided by RSD1 and RSD2). As the proton energy loss in these detectors was minimal the position resolution for these particles was limited to the 3 mm strip pitch of the DSSD.

The telescope was calibrated using an α-particle source and a secondary "cocktail" beam of mixed isotopes at five different magnetic rigidity settings of the LISE3 spectrometer. These covered the energy range of interest. The (FWHM) energy resolution was $\sim$ 200 keV for the silicon detectors and $\sim$ 1.5% for the CsI crystals. The average detector counting rates were 3.5 kHz (summed total for the 16 strips of RSD1), 4.3 kHz (summed total for the 16 strips of RSD2), 1.4 kHz (summed total for the 16 front and 16 back strips of the DSSD) and 190 Hz (summed total for the 64 CsI crystals). The higher rates in RSD1 and RSD2 reflect the flux of heavy isotopes (in this case Be and heavier) that were stopped in these detectors and not the DSSD or CsI array. The average data acquisition rate, triggered by events where 3 or more CsI crystals were active, was 140 Hz.

Events were selected for analysis based on the particle multiplicity (M) in the DSSD. Three categories were considered: M = 3 ($\alpha\alpha p$), M = 3 (αpp) and M = 4 ($\alpha\alpha pp$). The decay energy (E_{decay}) for each channel was reconstructed from the kinetic energies and momenta of the decay fragments: $\mathbf{P}_{parent} = \sum_{i=1}^{n} \mathbf{P}_{fragment_i}$ (n being the number of decay fragments), $E_{parent} = \mathbf{P}^2_{parent}/2m_{parent}$ (where m_{parent} is the mass of the decaying parent nucleus) and $E_{decay} = (\sum_{i=1}^{n} E_{fragment_i}) - E_{parent}$. The decay energy is related to the excitation energy (E_x) of the decaying nucleus via $E_x = E_{decay} - Q_n$, where Q_n is the n-body decay Q-value. This approach allows the excitation energy of a decaying nucleus to be determined without considering any intermediate (sequential) decay steps. For example, the excitation energy of ^{9}B may be obtained directly from the kinetic energies and momenta of the α+α+p decay fragments, without first reconstructing the initial p+^{8}Be decay. In this case m_{parent} is assumed to be 9, and Q_3, the 3-body decay Q-value, is the Q-value for the α+α+p decay of ^{9}B (278 keV).

In Fig. 1(a) the E_{decay} spectrum for the two α-particles in the M = 3 ($\alpha\alpha p$) channel is shown. A strong peak appears at the expected energy for the decay of the ^{8}Be$_{gs}$. This energy, Q_2 = 92 keV, is indicated by the arrow. The ^{8}Be$_{gs}$ events seen in Fig. 1(a) and the proton in the M = 3 ($\alpha\alpha p$) channel were then used to reconstruct E_{decay} for the ^{8}Be$_{gs}$+p decay of ^{9}B (Fig. 1(b)). Again the arrow indicates the expected ground state position, Q_3 = 278 keV. The cross-sections for the production of ^{8}Be$_{gs}$ and ^{9}B$_{gs}$ in the M = 3 ($\alpha\alpha p$) channel are given in Tab. I. These were calculated by correcting the experimental yields with detection efficiencies obtained from a Monte Carlo simulation of the reaction and detector array. The quoted uncertainties reflect both the statistical errors from the three target data sets and a 20 % uncertainty in the target thicknesses. The absolute cross-sections are also expected to be subject to a systematic uncertainty of the order of a factor of two. This arises as the angular distributions for each of the sequential decay processes are unknown. These have therefore been assumed to be isotropic in the centre-of-mass frame of the decays. The relative strength between the two channels is not very sensitive to the angular distributions used in the simulation, however, and is therefore not subject to such a systematic uncertainty. As may be seen in Tab. I, (72 ± 21) % of the ^{8}Be$_{gs}$ events seen in Fig. 1(a) arise from the decay of the ^{9}B$_{gs}$ events observed in Fig. 1(b).

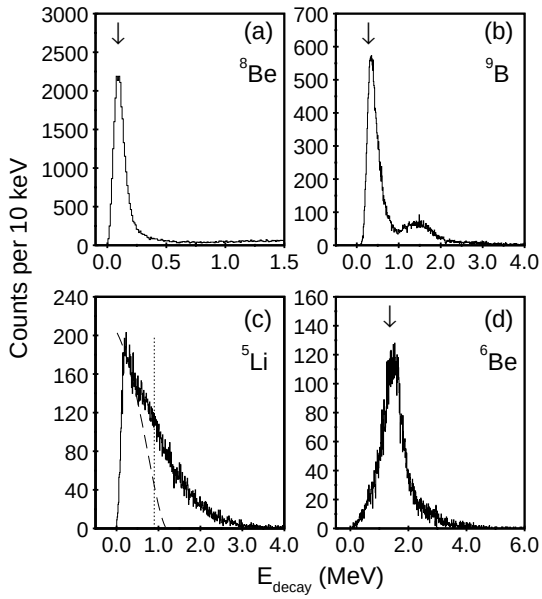

FIG. 1: Decay energy spectra for (a) ^{8}Be, (b) ^{9}B, (c) ^{5}Li and (d) ^{6}Be. The arrows indicate the known ground state energies. The various lines in (c) are described in the text.

In Fig. 1(c) the E_{decay} spectrum for the decay of ^{5}Li to α+p (Q_2 = 1967 keV) for M = 3 (αpp) events is shown. A clear peak at the ^{5}Li ground state energy is not seen, indicating little or no yield corresponding to direct α+p removal. However, the Q-value for the decay of ^{6}Be to

Multiplicity	Decay channel	σ (mb)
M=3 ($\alpha\alpha p$)	$^{8}\mathrm{Be_{gs}} \rightarrow \alpha + \alpha$	42.6 ± 8.8
M=3 ($\alpha\alpha p$)	$^{9}\mathrm{B_{gs}} \rightarrow {}^{8}\mathrm{Be_{gs}} + p$	30.5 ± 6.3
M=3 (αpp)	$(^{5}\mathrm{Li}_{(0-900\mathrm{keV})} \rightarrow \alpha + p)$	(17.4 ± 3.6)
M=3 (αpp)	$^{6}\mathrm{Be_{gs}} \rightarrow {}^{5}\mathrm{Li}_{(0-900\mathrm{keV})} + p$	10.5 ± 2.2
M=4 ($\alpha\alpha pp$)	$^{10}\mathrm{C} \rightarrow {}^{9}\mathrm{B} + p$	9.2 ± 1.9
M=4 ($\alpha\alpha pp$)	$^{10}\mathrm{C} \rightarrow {}^{6}\mathrm{Be} + \alpha$	3.3 ± 0.7

TABLE I: Cross-sections for the decay channels (see text).

^{5}Li+p is −595 keV, and hence the available $\mathrm{E_{decay}}(^{5}\mathrm{Li})$ corresponding to $^{5}\mathrm{Li_{gs}}$ decays is 1967 − 595 = 1372 keV. This decay proceeds via the tail of the ∼1.5 MeV wide $^{5}\mathrm{Li_{gs}}$. A calculation of the effect of the decay phase space and an l=1 centrifugal barrier indicates the yield from the decay is shifted away from 1372 keV towards $\mathrm{E_{decay}}(^{5}\mathrm{Li})$ = 0 keV, with 96 % of the $^{5}\mathrm{Li_{gs}}$ events being in the $\mathrm{E_{decay}}(^{5}\mathrm{Li})$ = 0 to 900 keV range. These calculations reproduce the sharp rise in the decay energy spectrum below 500 keV, the predicted decay strength (arbitrarily scaled) being indicated by the dashed line in Fig. 1c. Although the calculations do describe the data it is recognized that the width of the $^{5}\mathrm{Li_{gs}}$ is not well known, and there are possible α+p final state interactions. The cross-section for this channel is therefore not unambiguously determined, and hence is only given tentatively in Tab. I. A gate was applied across the 0 to 900 keV range (indicated by the vertical dotted line in Fig. 1(c)) to select the $^{5}\mathrm{Li_{gs}}$ events resulting from the decay of ^{6}Be. This gate maximised the $^{5}\mathrm{Li_{gs}}$ yield and at the same time minimized the background from M = 3 (αpp) events in which the $\mathrm{E_{decay}}(^{5}\mathrm{Li})$ was calculated from the α-particle and the incorrect proton.

In Fig. 1(d) the $\mathrm{E_{decay}}$ spectrum for ^{6}Be decay, obtained from the M = 3 (αpp) events and gated on the $^{5}\mathrm{Li_{gs}}$, is shown. The arrow indicates the expected ground state peak position ($\mathrm{Q_3}$ = 1372 keV). The observed peak indicates the analysis of the intermediate ^{5}Li decay was successful in selecting the correct events. Without the $^{5}\mathrm{Li_{gs}}$ gate the ^{6}Be $\mathrm{E_{decay}}$ spectrum contains increased background. The cross-sections for $^{5}\mathrm{Li_{gs}}$ and $^{6}\mathrm{Be_{gs}}$ production in the M = 3 (αpp) channel are listed in Tab. I, and are subject to the same factor of two systematic uncertainty as for the $^{8}\mathrm{Be_{gs}}$ and $^{9}\mathrm{B_{gs}}$ channels (see above). The cross-sections indicate that (60 ± 18) % of events within the 0 to 900 keV range of the ^{5}Li $\mathrm{E_{decay}}$ arise from $^{6}\mathrm{Be_{gs}}$ decay.

The ^{10}C $\mathrm{E_x}$ spectra, obtained from $\mathrm{E_x} = \mathrm{E_{decay}} - \mathrm{Q_4}$ ($\mathrm{Q_4}$ = −3.727 MeV) for the M = 4 ($\alpha\alpha pp$) events are shown in Fig. 2, along with the Monte Carlo predicted detection efficiencies (dot-dashed lines). To distinguish the ^{9}B+p and ^{6}Be+α decay channels a gate was applied to the ^{8}Be $\mathrm{E_{decay}}$ spectrum reconstructed from the two α-particles. This is not shown, but is very similar in form to that for the M = 3 ($\alpha\alpha p$) data (Fig. 1(a)). The ^{10}C

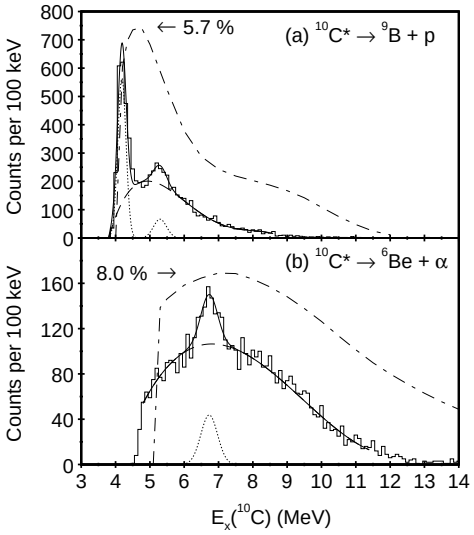

FIG. 2: $\mathrm{E_x}$ spectra for (a) ^{9}B + p and (b) ^{6}Be + α decay of ^{10}C. The various lines are described in the text.

$\mathrm{E_x}$ spectrum for events involving decay via the $^{8}\mathrm{Be_{gs}}$ is shown in Fig. 2(a) and corresponds to the $^{10}\mathrm{C} \rightarrow {}^{9}\mathrm{B} + p$, $^{9}\mathrm{B} \rightarrow {}^{8}\mathrm{Be} + p$, $^{8}\mathrm{Be} \rightarrow \alpha + \alpha$ decay channel. Events *not* decaying via the $^{8}\mathrm{Be_{gs}}$ are shown in Fig. 2(b). In order to minimize the contribution from decays to the ^{8}Be excited state at 3.04 MeV, an additional gate, on the $^{6}\mathrm{Be_{gs}}$, was applied to this data. The ^{6}Be $\mathrm{E_{decay}}$ spectrum for the M = 4 ($\alpha\alpha pp$) events is very similar in form to that for the M = 3 (αpp) data shown in Fig. 1(d). The data in Fig. 2(b) therefore correspond to the $^{10}\mathrm{C} \rightarrow {}^{6}\mathrm{Be} + \alpha$, $^{6}\mathrm{Be} \rightarrow {}^{5}\mathrm{Li} + p$, $^{5}\mathrm{Li} \rightarrow \alpha + p$ decay channel. The peaks observed in the spectra have been reproduced using Gaussian line shapes above a smooth (polynomial) background. The overall fits are given by the solid lines in Fig. 2, the background by the dashed lines, and the individual peaks by the dotted lines. Two peaks are seen at energies of (4.20 ± 0.01) and (5.31 ± 0.03) MeV and with widths of (280 ± 10) and (450 ± 90) keV (FWHM) respectively in Fig. 2(a). The peak at 4.20 MeV has not been previously reported and appears to be a new state in ^{10}C (it does not arise from any threshold effect). The second peak, at 5.31 MeV, corresponds to the known, and in this data, unresolved, states at 5.22 and 5.38 MeV [3]. In Fig. 2(b) one peak is seen at (6.74 ± 0.04) MeV with a width of (570 ± 110) keV. This corresponds to the known state at 6.58 MeV [3]. The observed widths are dominated by experimental resolution, which is proportional to $(\mathrm{E_x} - \mathrm{E_{threshold}})^{1/2}$. A resolution of 280 keV at 4.2 MeV would rise to 650 keV at 6.7 MeV following this relationship. The uncertainties quoted in the centroid energies are statistical only. A 200 keV uncertainty across the observed $\mathrm{E_x}$ range is typical in breakup work of this kind. The cross-sections for the ^{9}B+p and ^{6}Be+α breakup of ^{10}C are given in Tab. I. These were obtained by determining the experimental yields over a range of

E_x (MeV)	Decay channel	σ (mb)
4.20 ± 0.01	^{9}B + p	2.9 ± 0.6
5.31 ± 0.03	^{9}B + p	0.45 ± 0.22
6.74 ± 0.04	^{6}Be + α	0.46 ± 0.19

TABLE II: Cross-sections for the ^{10}C excited states.

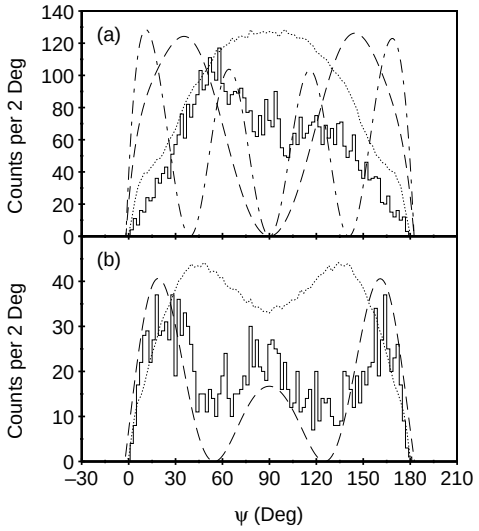

FIG. 3: Angular distribution (ψ) for the (a) 4.20 and (b) 5.31 MeV states in ^{10}C. The various lines are described in the text.

excitation energies (starting at the decay threshold), 4.0 to 7.0 MeV in the case of the ^{9}B+p decay and 5.1 to 12.0 MeV for the ^{6}Be+α channel. Cross-sections for the individual states observed in Fig. 2 are listed in Tab. II.

The structure of the ^{10}C ground state is, in principle, probed via the α and p-removal processes. Tab. I lists the corresponding cross-sections for the M = 3 and 4 final states. The two multiplicities probe different types of reaction processes. The M = 4 yields reflect "diffractive" breakup, whereas the M = 3 also include absorptive processes, where either the proton or α-particle is "absorbed" by the target. Correspondingly, the M = 3 cross-sections are larger than the M = 4 counterparts. In both the M = 3 and 4 data the ^{9}B+p cross-section is $\sim$ 3 times larger than that for the ^{6}Be+α breakup. It should be noted that the probability of the disintegration of an initial state α-particle is small due to the high breakup threshold of ^{4}He (19.8 MeV). Thus the favouring of the proton removal correlates with the lower breakup threshold for that channel (Q[^{10}C $\rightarrow$ ^{9}B + p] = $-$4.005 MeV) compared with α-removal (Q[^{10}C $\rightarrow$ ^{6}Be + α] = $-$ 5.099 MeV). From a clustering perspective, the lower p-decay threshold would permit the ^{9}B+p configuration to be more strongly developed in the ground state than the ^{6}Be+α partition.

In Fig. 3 angular distributions are shown for the 4.20 and 5.31 MeV states observed in the ^{9}B+p decay of ^{10}C. Here ψ corresponds to the angle between the relative velocity vector of the ^{9}B and p decay fragments and the beam axis. The dotted lines indicate the predicted angular distributions obtained from a Monte Carlo simulation assuming isotropic decay. In Fig. 3(a), the ψ distribution for the 4.20 MeV state, there appears to be little structure, although there is some evidence that the distribution has a minima at $\psi = 90°$. This suggests that the data should be described by an odd order Legendre Polynomial. Monte Carlo efficiency corrected Legendre Polynomials of order 1 (dashed line) and 3 (dot-dash line) are shown, but it is clear that neither provides a good description of the experimental yield. The angular distribution for the 5.31 MeV state (Fig. 3(b)) exhibits a much clearer periodic structure, and there is a very good agreement with the Monte Carlo corrected Legendre Polynomial of order 2 (dashed line).

The spectrum of ^{10}C excited states should closely mirror that of ^{10}Be (the latest work is summarised in Ref. [4]). In the present region of interest there are four states which are almost degenerate in ^{10}Be: 5.958 MeV [2^+], 5.960 MeV [1^-], 6.179 MeV [0^+] and 6.263 MeV [2^-]. The negative parity states correspond to the excitation of a $p_{3/2}$ neutron to the sd-shell, and the 2^+ state to the recoupling of the p-shell nucleons [5]. The equivalent states in ^{10}C should be strongly populated in the ^{10}B(^{3}He,t)^{10}C reaction [6]. The 6.179 MeV [0^+] state in ^{10}Be corresponds to a $(sd)^2$ configuration. This state has recently been shown to possess a highly deformed α+2n+α structure [7]. The states observed in the ^{10}B(^{3}He,t)^{10}C reaction, at 5.22, 5.38 and 6.58 MeV [6], were also observed in the inelastic scattering studies recently reported in Ref. [8]. It is likely that these correspond to the 1^-, 2^- and 2^+ states. The 4.20 MeV state was not observed in Ref. [8], however, although this may be due to a reduced detection efficiency at low E_x when compared to the present work. In the current data set the 4.20 MeV state was only seen after "pileup" events in the DSSD were recovered. Such events occur in low E_{decay} breakup, where the small relative laboratory angle between particles often leads to detection of two (or more) particles in the same front DSSD strip but separate back DSSD strips (or vice versa). As the individual particle energies are known from the separate strips from the side of the DSSD where pileup did not occur the event may be reconstructed. Recovery of such events, where the DSSD front and back multiplicities do not both equal M = 4, gave rise to very good detection efficiency at low values of E_x. The 4.20 MeV peak was not strongly populated (if at all) in the charge-exchange reaction [6], indicating that it is associated with a more complex configuration, perhaps $(sd)^2$. The angular distributions (Fig. 3) for the 4.20 and 5.31 MeV peaks are characteristically different, indicating different spins. The subsequent proton decay of a 1^- (2^-) state would proceed through l-values of 0, 2 (0, 2, 4). A 0^+ state would decay via l=1. Interestingly, the data for the 5.31 MeV peak suggests l=2, indicating the

peak is associated with the 1^- or 2^- states. The angular distribution for the 4.20 MeV peak, however, indicates odd l, suggesting an association with the 0^+ state. The 6.74 MeV state in ^{10}C could then be the analogue of the 5.958 MeV [2^+] state in ^{10}Be.

If the 4.20 MeV state is the analogue of the 6.179 MeV 0^+ molecular state in ^{10}Be [7], it would be expected that the two states should lie at approximately the same energy above the respective cluster decay thresholds. In the case of ^{10}Be, the 0^+ state lies 0.6 MeV below the ^{9}Be+n decay threshold, whereas the ^{10}C 4.20 MeV state lies 0.2 MeV above the ^{9}B+p decay threshold. This relatively small difference could arise from the increased repulsion in the case of ^{9}B+p. It is possible to calculate the Coulomb energy difference (CED) expected between such molecular states in ^{10}Be and ^{10}C. If the present 4.20 MeV state is indeed associated with the 6.17 MeV ^{10}Be state, then the energy difference is close to 2 MeV. Such a difference is rather large compared to other nuclei but could be enhanced for an extended distribution of the valence particles. The CED of the ^{10}Be and ^{10}C ground-states was computed according to the formalism from Ref. [9]

$$E_c = \left[0.60Z^2 - 0.460Z^{4/3} - 0.15(1-(-1)^Z)\right] e^2/R \quad (1)$$

where E_c is the Coulomb energy and $R=1.3A^{1/3}$. The energy difference of the excited states was calculated assuming a ^{4}He+^{6}He(^{6}Be) cluster partition with a separation of 5.9 fm. This separation is that deduced in Ref. [4] from an analysis of the rotational band based on the 0^+_2 state in ^{10}Be. Such an analysis gives an energy shift of 0.8 MeV (i.e. $E_x(^{10}C)$=5.37 MeV). However, since the two protons are localized at one center, this has a higher energy than two ^{5}Li clusters with the same separation, with a radius given by $R=1.3A^{1/3}$. In this instance, a reduction of 1.45 MeV in the energy of the 0^+ excited state is found, $E_x(^{10}C)$=4.72 MeV. Furthermore, if the valence protons are allowed to occupy extended orbits outside the α-particle cores then the Coulomb energy, and therefore the excitation energy, would be reduced. The Coulomb energy of two concentric spheres of differing radii was calculated in Ref. [10]. With a molecular description of the excited state, the valence particles are exchanged between the α-particle cores. In this instance, the valence protons/neutrons would have a radius approaching the separation of the α-particles. This would induce a Coulomb shift of 1.85 MeV, and place the 0^+ state close to 4.3 MeV – consistent with the present measurement. Of course, the present estimates ignore the exchange properties and correlations which may exist in the system and assume spherical distributions. Calculations based or more microscopic approaches would be interesting.

In summary, both the ground state structure and that of the excited states has been explored in the present measurements. The dissociation of the ground state of the Brunnian nucleus ^{10}C into the constituents $2\alpha + 2p$ has been measured. The cross-sections indicate that the dominant configuration is ^{9}B+p, rather than ^{6}Be+α. In the multiplicity 4 coincidences, the ^{10}C excitation energy spectra have been reconstructed. A new state was observed at E_x = 4.20 MeV, which may be the α+2p+α analogue of the 6.179 MeV [0^+] α+2n+α molecular state in ^{10}Be. It should be noted that the ground and excited states should have different structures, based on the understanding which has been developed for ^{10}Be [4]. The ground state is expected to be more compact. A calculation of the energy difference between the ground and excited states in ^{10}Be and ^{10}C shows that, in order to produce a 0^+ state at 4.20 MeV, a large degree of clusterization is required and that the protons should occupy delocalised orbits.

The assistance of the GANIL and LPC technical staff is gratefully acknowledged. This work has been supported by the European Community FP6 - Structuring the ERA - Integrated Infrastructure Initiative - contract EURONS n° RII3-CT-2004-506065.

* Email: n.curtis@bham.ac.uk

[1] M.V. Zhukov, B.V. Danilin, D.V. Fedorov, J.M. Bang, I.J. Thompson and J.S. Vaagen, Phys. Rep. **231**, 151 (1993).
[2] H.Brunn, Über Verkettung, S.-B.Math.-Phys.Kl. Bayer Akad. Wiss. **22**, 77 (1892).
[3] D.R. Tilley, J.H. Kelley, J.L. Godwin, D.J. Millener, J.E. Purcell, C.G. Sheu and H.R. Weller, Nucl. Phys. **A745**, 155 (2004).
[4] H.G. Bohlen, T. Dorsch, Tz. Kokalova, W. von Oertzen, Ch. Schulz and C. Wheldon, Phys. Rev. C **75**, 054604 (2007).
[5] W. von Oertzen, Z. Phys. A **354**, 37 (1996).
[6] M.J. Schneider, B.W. Ridley, M.E. Rickey, J.J. Kraushaar and W.R. Zimmerman, Phys. Rev. C **12**, 335 (1975).
[7] M. Freer, E. Casarejos, L. Achouri, C. Angulo, N.I. Ashwood, N. Curtis, P. Demaret, C. Harlin, B. Laurent, M. Milin, N.A. Orr, D. Price, R. Raabe, N. Soić, and V.A. Ziman, Phys. Rev. Lett. **96**, 042501 (2006).
[8] R.J. Charity, K. Mercurio, L.G. Sobotka, J.M. Elson, M. Famiano, A. Banu, C. Fu, L. Trache and R.E. Tribble, Phys. Rev. C **75**, 051304(R) (2007).
[9] S. Shlomo, Rep. Prog. Phys. **41**, 957 (1978).
[10] K. Wildermuth and Y.C. Tang, A Unified Theory of the Nucleus (Vieweg, Braunschweig, Germany, 1977), p. 322.

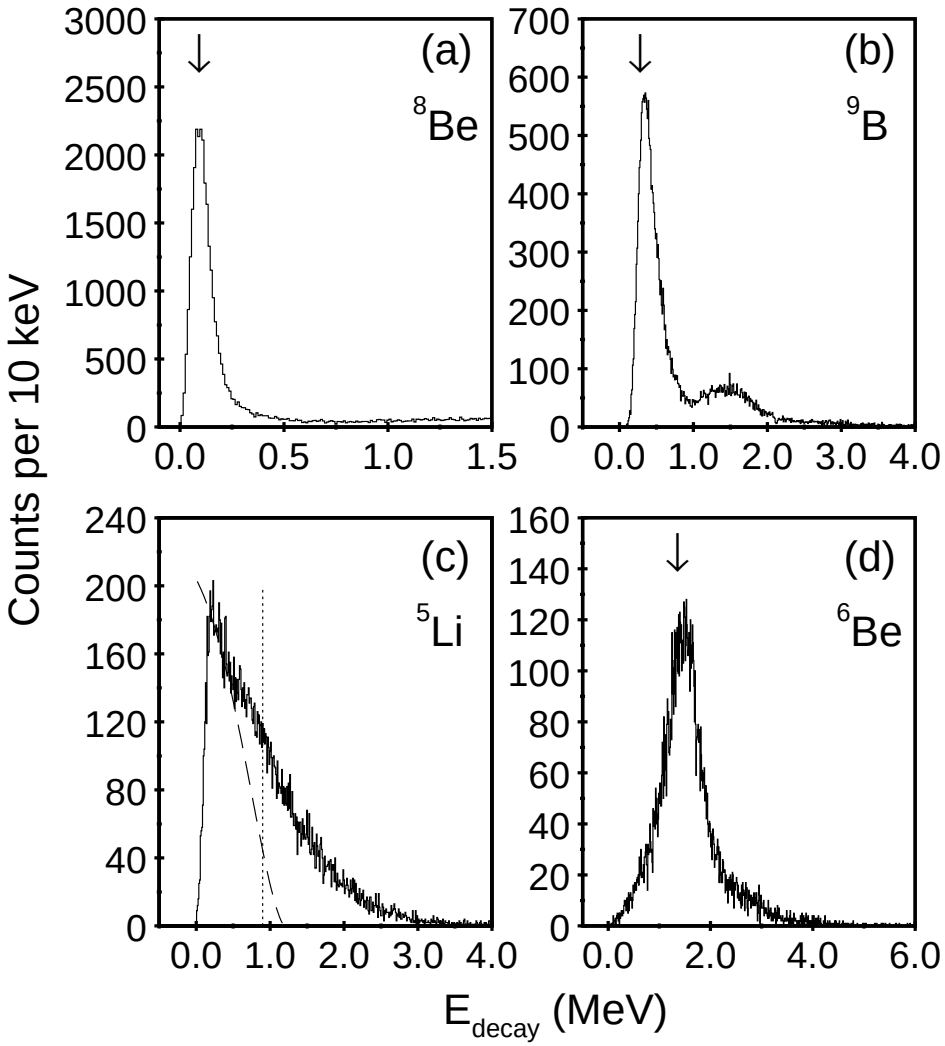

Figure 1

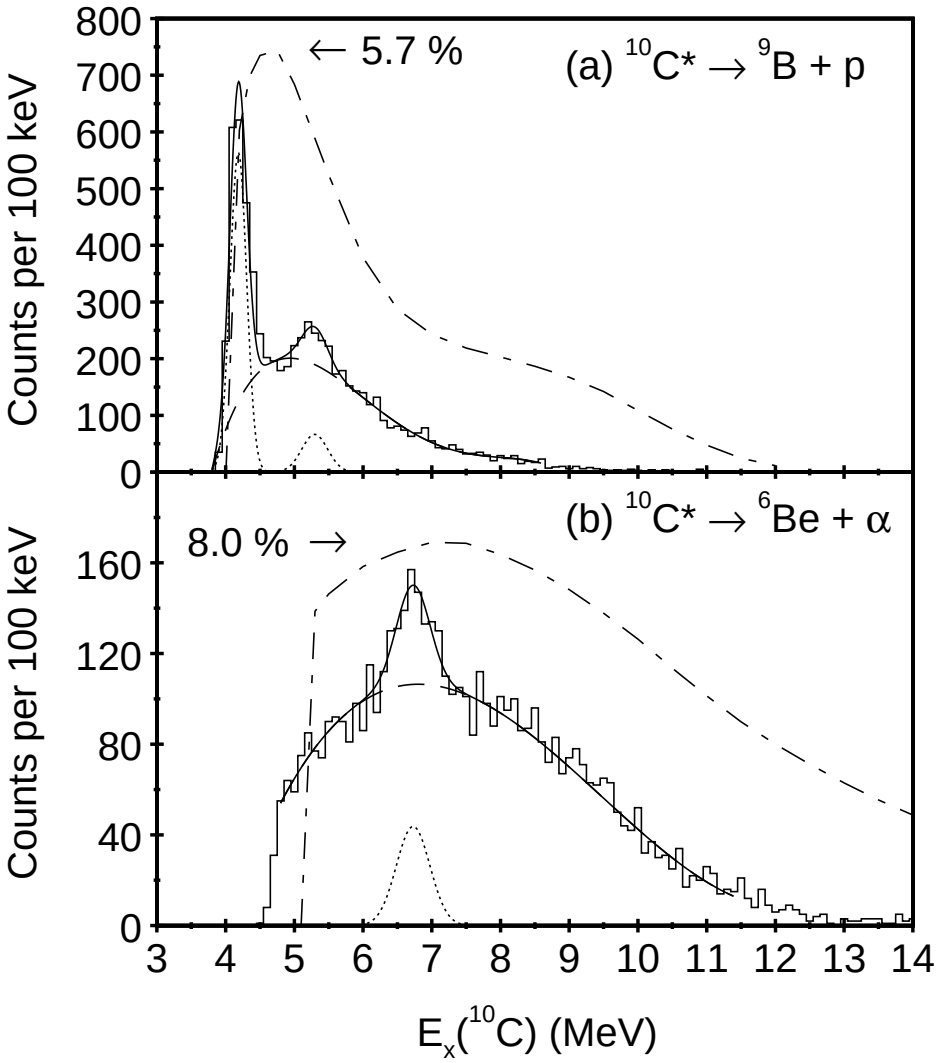
800
700
600
500
400
300
200
100
0
Counts per 100 keV
← 5.7 %
(a) $^{10}C^* \rightarrow {}^{9}B + p$
160
120
80
40
0
Counts per 100 keV
8.0 % →
(b) $^{10}C^* \rightarrow {}^{6}Be + \alpha$
3 4 5 6 7 8 9 10 11 12 13 14
$E_x(^{10}C)$ (MeV)

Figure 2

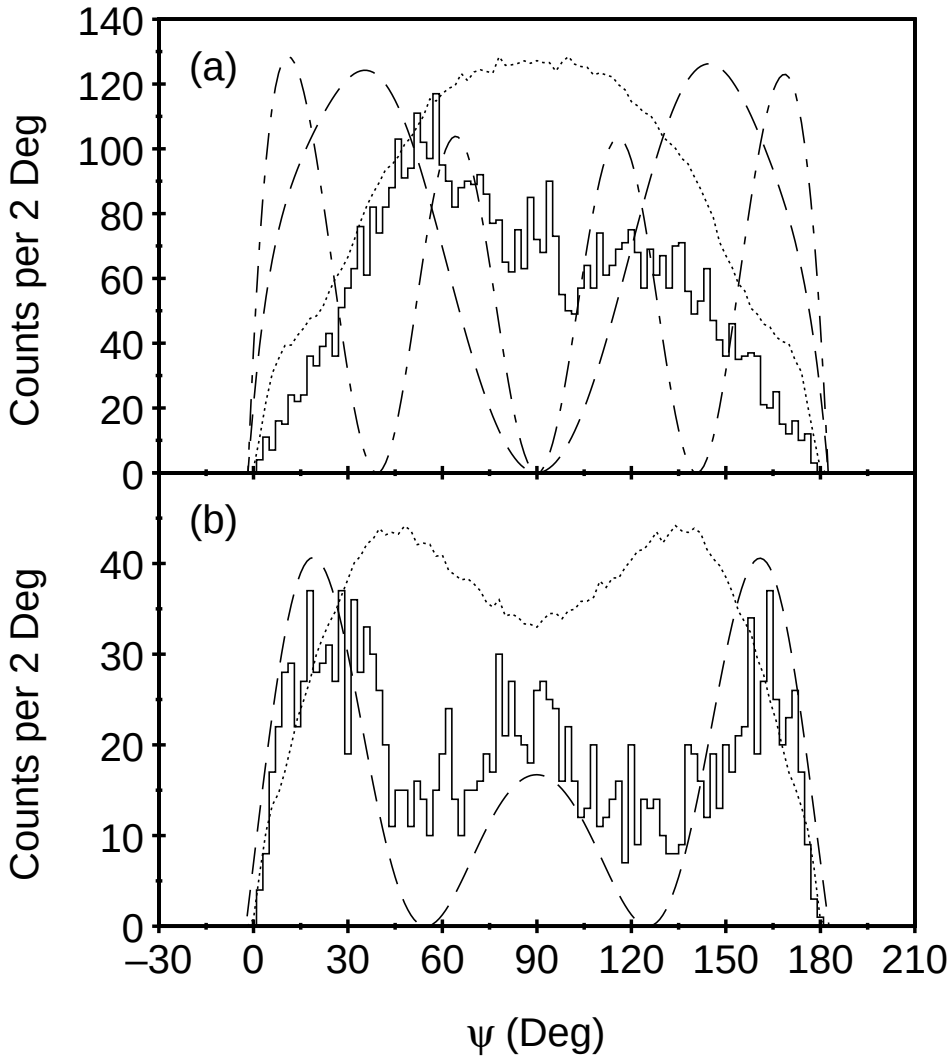
(a)
(b)
Counts per 2 Deg
Counts per 2 Deg
140
120
100
80
60
40
20
0
40
30
20
10
0
–30
0
30
60
90
120
150
180
210
ψ (Deg)

Figure 3